JOURNAL OF GEOPHYSICAL RESEARCH, VOL. 101, NO. D21, PAGES 26,479–26,491, NOVEMBER 27, 1996

Scalar multifractal radar observer's problem

S. Lovejoy and M.R. Duncan
Physics Department, McGill University, Montreal, Quebec, Canada

D. Schertzer
Laboratoire de Météorologie Dynamique (CNRS), Paris, France

Abstract. The classical radar observer's problem in rain is to interpret the fluctuating radar echo from precipitation. Contrary to the usual homogeneity assumption involving Poisson statistics and incoherent scattering, we make a (scaling) heterogeneity assumption involving multifractal statistics and (some) coherent scattering. We consider the simplest problem, which is to relate the liquid water (σ) statistics to the (measured) effective radar reflectivity statistics (Z_e) and to the (theoretical) radar reflectivity factor (Z; Z_e=Z for incoherent scattering). We ignore polarization effects (that is, we use the scalar wave approximation), and denote the pulse length l, wavelength λ_w, the inner (homogeneity) scale of the rain field (η), and the outer (largest) scale of rain (L). For the simplest (conservative) multifractal σ the two main effects are 1) as in the standard theory, $Z \approx \sigma^2$; however, because of the strong subpulse volume gradients, there is a bias of $(l/\lambda_w)^{K\sigma(2)}$; ($K_\sigma(2)$ is the scaling exponent of σ^2); 2) because of partial coherence, there is an enhancement: $Z_e/Z \approx (\lambda_w/\eta)^{D-K\sigma(2)}$, where D is the (effective) dimension of space. For nonconservative multifractals (parametrized by H) we obtain the overall bias in the means: $\langle Z_e \rangle / \langle Z \rangle \approx (\lambda_w/\eta)^{D-K\sigma(2)}(L/\lambda_w)^{-2H}$. Using available data, we estimated this as typically $\approx 10^{-3}$ which is $<<1$; Z should therefore not be used as a proxy for Z_e. New theories relating radar measurements to rain must therefore be developed. Finally, we show that radar "speckle" (the drop "rearrangement" problem) is a general consequence of multifractal liquid water/ drop correlations.

1. Introduction

The standard interpretation of the fluctuations of radar echoes from precipitation is based on the implausible assumption that, although interesting and significant inhomogeneities do exist at (observed) scales larger than the pulse volume, each realization of the rain field is statistically homogeneous within the pulse volume. More specifically, it is assumed that within pulse volumes the probability density of finding a drop is uniform in space, hence that the statistics are Poisson and that the reflected microwave phases are independent random variables. This implies completely incoherent scattering. Since a uniform probability still allows for some residual variability of the size and exact positions of drops, the radar echo will still fluctuate, leading to a statistical description which has served for over 40 years and which we term "the standard model" [see *Lawson and Uhlenbeck*, 1950; *Austin*, 1952; *Marshall and Hitschfeld*, 1953; *Wallace*, 1953]. The homogeneity assumption originated as the simplest one that would allow calculation of "burn through" times for detecting military targets in metal chaff or rain [*Lawson and Uhlenbeck*, 1950]. Until recently, little evidence was found to contradict this model [see *Lhermitte and Kessler*, 1966; *Schaffner et al.*, 1980]. A limited attempt to go beyond strict homogeneity was made by *Rogers*, [1971] (see also [*Torlaschi and Humphries*, 1983]) who formulated a modification to the statistical description of the fluctuating echo that permits rain rate gradients within an extended measurement or averaging volume (scale > radar measurement or pulse volume) while retaining the assumption that the rain field is homogeneous at scales below the resolution of the radar. This treatment of inhomogeneity still separates the physics of the rain field along the arbitrary line separating subradar-resolution scales from superradar-resolution scales.

The development of high-speed recording and processing has now made it possible to digitize every single pulse and perform sophisticated analyses down to scales of milliseconds and meters, showing that the variability is large down to these small scales. Radar-based studies of the scaling properties of the effective radar reflectivity go back to the early 1980s [*Lovejoy*, 1981, 1983; *Lovejoy and Mandelbrot*, 1985; *Schertzer and Lovejoy*, 1985, 1987; *Lovejoy et al.*, 1987; *Gabriel et al.*, 1988; *Gupta and Waymire*, 1990, 1993; *Tessier et al.*, 1993]. Other studies based on gage data [*Hubert et al.*, 1993; *Ladoy et al.*, 1993; *Tessier*, 1993; *Tessier et al.*, 1993, 1995; *Fraedrich and Larnder*, 1993; *Olsson*, 1995, 1996; *Olsson and Niemczynowicz*, 1996; *Svensson et al*, 1996] support these findings at scales of minutes to hours, days and weeks, whereas lidar and blotting paper experiments support this over the range of scales ≈500 m down to ≈2-3 mm [*Lovejoy and Schertzer*, 1991, 1990a] respectively; see *Lovejoy and Schertzer*, [1995b] for a review. This small inner scale was roughly equal to the mean interdrop distance over the experimental region 128X128 cm^2. These studies have contributed to the mounting evidence in the literature that rain and other turbulent atmospheric fields respect a symmetry principle known as scale invariance or scaling. This is consistent with the classical idea that turbulent cascades concentrate energy and other conserved fluxes into smaller and

Copyright 1996 by the American Geophysical Union.

Paper number 96JD02208.
0148-0227/96/96JD-02208$09.00

smaller volumes. The nonclassical result of such cascades is a special type of extreme variability associated with multifractal statistics.

The multifractal model provides a scale invariant alternative to the scale breaking of the physics implied by the standard theory. This model also provides a precise form for the description of sub-radar-resolution variability in the rain field. Further, many of these studies reveal that the multiscaling behaviors are well described by the universal multifractal formalism of *Schertzer and Lovejoy* [1987, 1989, 1996a,b], *Schertzer et al.* [1991, 1995]; *Brax and Pechanski* [1991]; *Kida* [1991] in which the multiscaling is determined by only three parameters. A multiscaling model implies that subresolution and superresolution variability are statistically related only via the ratio of scales (note that the notion of scale itself need not be isotropic; see below). We can therefore exploit the observations of multiscaling at superresolution scales in order to create a potentially realistic model of the subresolution variability. *Duncan et al.* [1992], *Duncan* [1993], and *Tessier et al.* [1993] showed that rain field gradients exist down to the resolution scales of a radar, which for these studies was approximately 40 m (which would be subresolution for many weather radar systems). Furthermore, they showed that the gradients are multiscaling and argue that this behavior will extend to the smallest scales of the rain field.

This observational evidence supporting a multiscaling model of the rain field suggests a quite different picture than that presented in the standard theory. Instead of the requirement that the rain field be homogeneous below the (arbitrary) measurement scale with significant gradients only above that scale, we can expect the presence of large gradients/variability at all scales but with the condition that a priori no scales dominate. Some of the implications of the scaling variability on effective reflectivity factors have already been considered in the literature. For example *Lovejoy and Schertzer* [1990a] showed that the observed small-scale clustering, when modeled by a single fractal dimension (the "monofractal approximation"), would lead, via the implied partial coherence effects, to systematic biases. Finally, *Lovejoy and Schertzer* [1990b] showed that the observed large-scale multifractal variability is far larger than the standard theory's exponential variability of effective radar reflectivity factor Z_e with regard to the reflectivity factor Z.

Boiled down to its essentials (ignoring beam pattern and other geometric effects) and assuming a scalar wave (ignoring polarization effects) the amplitude found at the radar's receiver is a Fourier component of the rain field within the pulse volume. For the particularly simple case where the liquid water density is a conserved multifractal (i.e. the direct result of a multifractal cascade), we calculate Z_e for both coherent and incoherent models of subgrid variability. In the more physically realistic case where it is a nonconserved multifractal (modeled as a fractional integral of a conserved flux), we calculate a "bias" in the mean reflectivity factors $\langle Z_e \rangle / \langle Z \rangle$, which by using available empirical evidence, we find $\ll 1$. This result brings into question the relevance of the essentially theoretical quantity Z for interpreting radar data.

In section 2 we discuss the multifractal model and relate the usual (particle based) definitions of Z and Z_e to continuous field-based definitions which are equivalent for scales larger than the mean interdrop distances. The use of integrals over continuous fields rather than discrete sums enables us to directly use the conventional multifractal (codimension) formalism where the statistics are determined by the moment-scaling function (or equivalently by the codimension function) which specifies how the cloud liquid water statistics change with scale. The third part gives the details of the calculation (including numerical tests) of the statistics of Z, Z_e for incoherent, coherent, and multifractal subpulse volume variability (various calculational details are given in the appendix). Also included is a discussion of the multifractal origin of radar "speckle" which in this case corresponds to the sensitivity of Z_e to subpulse volume "drop rearrangement." The origin of this effect as a singularity in the multifractal autocorrelation functions is quite general and will probably lead to applications in radar problems involving multifractal surface targets (rather than just the volume-distributed targets discussed here). Finally, section 4 compares the results with limited liquid water and radar rain data and discusses the significance of the results.

2. Multifractal Representation of Liquid Water and Reflectivity

2.1. Physical Basis of Multiscaling in Rain

Rainfall is nonlinearly coupled with the wind, temperature, and other atmospheric fields; it is therefore a turbulent process. Multiscaling (or equivalently multifractal) models of turbulence appeal to three aspects of turbulence: 1) their scale invariance down to a small inner "dissipation" scale, 2) their (scale by scale) conservation properties (e.g., of energy flux, passive scalar variance flux; more precisely, if ε_λ is the conserved energy flux at scale/resolution λ, then conservation means $\langle \varepsilon_\lambda \rangle$=constant; independent of λ 3) the concept of a cascade which follows if in addition to aspects 1, and 2 there is "locality" in Fourier space (that is the strongest interactions occur between structures of similar sizes; this may be quite nonlocal in real space!). The generic outcome of such cascades is a highly intermittent/variable multifractal field with certain rather specific properties, including the existence of fractal structures and singularities of all orders (manifested through structures and clustering at all scales).

The notion of the rain field modeled as a cascade is quite different from that associated with the standard Poisson model. For instance, a multiscaling liquid water density field σ has longrange correlations. Small scales are hierarchically dependent on larger scales. This leads to the following variation of the q^{th} order statistical moment with resolution λ

$$\left\langle \sigma_\lambda^q \right\rangle = \lambda^{K_\sigma(q)} \tag{1}$$

where $K_\sigma(q)$ is the (convex) moment scaling function (in the case where K_σ is linear, σ is monofractal, not multifractal; for conservative processes, $K_\sigma(1)=0$). The angle brackets "<.>" indicate statistical (ensemble) averaging. This picture of the rain field can be justified by appeal to the concept of eddies in turbulence theory. In a scaling regime there is continuity of the physical processes across a wide range of scales. Thus over the scaling range the division of the rain field into different scale ranges is essentially arbitrary.

2.2. Scales and Scale Ratios, the Representation of Radar Quantities by Continuous Fields

There are four scales which we must consider (see Table 1 for a summary). The first two are properties of the rain field itself: the inner and outer scale of the scaling regime. The inner

Table 1 Summary of Length Scales and Dimensionless Ratios used in Text

Quantity	Typical Value	Symbol	Scale ratio	Typical ratios
Outer scale of rain	10^3 - 10^4 km	L	1	1
Inner rain scale	≈ interdrop distance ≈ 1cm, light-rain	η	Λ	10^8-10^9
Radar pulse length	100 m - 1 km	l	λ	10^4
wave-length	3 - 10 cm	λ_w	k_r	10^7-10^8

scale, denoted η, is the smallest scale of inhomogeneity/largest scale of homogeneity. The symbol η comes from the turbulence literature where it represents the turbulent dissipation scale (which is of the order of millimeters) and which is apparently comparable to the inner scale of moderate rain [see e.g., *Lovejoy and Schertzer*, 1990a; *Duncan*, 1993]. Just as the turbulent dissipation scale depends on the overall intensity of the turbulence, η will depend on the rain rate; it is at least as large as the mean interdrop distance. The outer scale, denoted L, is the largest scale in the scaling regime; according to the global rain gage data analyzed by *Tessier et al.* [1993] (in conjunction with other data such as cloud and aircraft data [*Lovejoy et al.*, 1993; *Lovejoy and Schertzer*, 1995a]), this is apparently of the order of the size of the Earth, although as long as it is larger than the pulse scale, its exact value is not too important. The radar measurement process clearly involves two further lengths: the pulse length l and the wavelength λ_w (the subscript "w" is used to avoid confusion with the scale ratio λ introduced below). We shall see that the results of radar measurements depend greatly on whether the inner scale is larger or smaller than the wavelength scale; for typical weather radars we note l≈100 m-1 km, λ_w≈3-10 cm, so that we have $L>>l>>\lambda_w$. Since even relatively low rain rates have interparticle distances of the order of a centimeter, we also take $\lambda_w>\eta$. Furthermore, in a scaling regime, only scale ratios are important; we therefore nondimensionalize all the lengths using the outer scale; this leads to define the following scale ratios: $\lambda=L/l$, $k_r=\pi L/\lambda_w$, $\Lambda=L/\eta$ with $1<<\lambda<<k_r<\Lambda$. Note that in isotropic systems, k_r is (twice) the modulus of the (non dimensional) wave vector representing the radar pulse direction and wave number (see below for the necessary anisotropic extensions accounting for differential stratification and rotation of structures). The factor of two is introduced for convenience to take into account the round trip of the wave from the radar to rain drop and back; see equation (2) below. It will also be convenient to introduce the non dimensional position vector $\boldsymbol{x}=\boldsymbol{r}/L$ where r is the usual position vector with the radar at the origin. To avoid confusion, all these ratios are inversely proportional to the corresponding distances.

We now discuss the representation of the rain field. Even assuming spherical drops and a scalar wave equation (i.e., ignoring polarization effects), a complete representation of the rain field involves specifying the position, size, and velocity of each drop. In this paper we will relate the drop volume statistics to the reflectivity statistics and hence we will not require the velocity. Since we anticipate that the drops will respond sensitively to their turbulent environment, a solution of the full rain rate/reflectivity problem will of necessity involve assumptions about the coupled velocity/drop volume cascades (we do not make the usual but unrealistic assumption that the drops always fall at their asymptotic free-fall rate). The appropriate theoretical framework for such coupled cascade processes is Lie cascades [*Schertzer and Lovejoy*, 1995]; this full problem will be developed elsewhere. Our aim is limited to relating the statistics of liquid water with radar measured quantities.

Consider the radar scan to be composed of a large number of pulse volumes (B_λ), resolution λ; the notation "B_λ" denotes a "ball" scale ratio λ. We ignore geometric radar antenna factors, and constant factors such as the dielectric constant, and we neglect the variation of the $1/r^2$ range dependence of the wave amplitude across the pulse volume. We now recall that the electric field due to the microwave-induced polarization is linearly proportional to the drop volume (V). We therefore find that the (complex) radar-scattered field is proportional to

$$A_\lambda(\boldsymbol{k}_r) = \frac{1}{\mathrm{vol}B_\lambda} \sum_{j\in B_\lambda} V_j e^{i\boldsymbol{k}_r\cdot\boldsymbol{x}_j} \tag{2}$$

where the sum is over the drops (indexed by j) in the pulse volume. Also, as indicated earlier, we have absorbed the round trip factor 2 into the definition of $\boldsymbol{k}_r$. Note that the actual measured, real signal, is obtained as usual by adding the complex conjugate to the above. The proportionality constant depends on the dielectric constant which we assume fixed (we do not consider temperature effects). Note that we also assume that the scattered wave is in phase with the incident wave; that is, we ignore absorption. The notation $\mathrm{vol}B_\lambda = \lambda^{-D}$ indicates the (nondimensional) volume of the (pulse volume) set B_λ. In usual isotropic spaces, D is the usual dimension of space, i.e., 3 for volumes, 2 for planes, 1 for lines. However, because of gravity, rain is an anisotropic scaling system and we must replace D by the effective "elliptical" dimension (*Lovejoy et al.* [1987] estimated this as D=2.22±0.07 in effective radar reflectivity fields; see below for more details). Although some more details of the formalism "generalized scale invariance" (GSI) are given below, readers are refered to *Schertzer and Lovejoy* [1985, 1987], and *Pecknold et al.* [1993, 1995]. For those with no familiarity with GSI, use of D=3 everywhere will suffice for understanding the main ideas.

The basic parameter measured by a weather radar is the intensity of the return signal from which one deduces the effective reflectivity factor ($Z_{e,\lambda}$), (we ignore polarization effects; hence we do not consider differential reflectivity). After removing all the geometric (antenna and distance dependent) factors, $Z_{e,\lambda}$ is given by

$$Z_{e,\lambda} = \frac{1}{\mathrm{vol}B_\lambda} \left| \sum_{j\in B_\lambda} V_j e^{i\boldsymbol{k}_r\cdot\boldsymbol{x}_j} \right|^2 \tag{3}$$

We also introduce the traditional radar reflectivity factor Z_λ:

$$Z_\lambda = \frac{1}{\mathrm{vol}B_\lambda} \sum_{j\in B_\lambda} V_j^2 \tag{4}$$

The standard radar theory is now recovered by assuming that the variance of V is finite and that the scattering is totally incoherent. In this case, the phases in equation (3) are

independent identically distributed random variables and for a large number of drops, the cross terms cancel leading to $Z_{e,\lambda} \approx Z_\lambda$. A more precise result taking into account the fluctuation of Z_e about the mean Z can be obtained [*Marshall and Hitschfeld*, 1953; *Wallace*, 1953] for the conditional probability of measuring Z_e, given Z

$$p(Z_e|Z) = \frac{1}{Z} e^{-Z_e/Z}$$

However, the exponential variation of Z_e about Z is much smaller than the multifractal variability considered here and will be ignored (see *Lovejoy and Schertzer*, [1990b] for more details).

2.3. Liquid Water and Radar Quantities As Densities of Continuous Fields

To express our results in terms of the usual multifractal densities (rather than in terms of drop volumes at well-defined positions as above), we now introduce the liquid water density at resolution λ:

$$\sigma_\lambda = \frac{1}{\mathrm{vol}B_\lambda} \sum_{j \in B_\lambda} V_j \tag{5}$$

where the sum is (as above) over all the drops in B_λ. If the radar volume is covered by disjoint balls B_λ, then $\sigma_\lambda(\boldsymbol{x})$ is a (piecewise) continuous density field at scale ratio λ (size=L/λ).

Now consider an inner scale Λ smaller than the wavelength and small enough so that a typical volume element rarely contains more than one drop: $\sigma_\Lambda = V/\mathrm{vol}B_\Lambda$. We can now express A, Z, Z_e in terms of the continuous field $\sigma_\Lambda(\boldsymbol{x})$. For example, for a scale $\lambda < \Lambda$ we have

$$Z_\lambda = \frac{\mathrm{vol}B_\Lambda}{\mathrm{vol}B_\lambda} \int_{B_\lambda} \sigma_\Lambda^2(\boldsymbol{x}) d\boldsymbol{x} \tag{6}$$

Similarly, the scattering amplitude field A_λ is

$$A_\lambda = \frac{1}{\mathrm{vol}B_\lambda} \int_{B_\lambda} \sigma_\Lambda(\boldsymbol{x}) e^{i\boldsymbol{k}_r \cdot \boldsymbol{x}} d\boldsymbol{x} \tag{7}$$

and the effective reflectivity field $Z_{e,\lambda}$ is

$$Z_{e,\lambda} = \frac{1}{\mathrm{vol}B_\lambda} \left| \int_{B_\lambda} \sigma_\Lambda e^{i\boldsymbol{k}_r \cdot \boldsymbol{x}} d\boldsymbol{x} \right|^2 \tag{8}$$

From equations (6), (7), we find the following relation between the effective reflectivity factor and the scattered field amplitude:

$$Z_{e,\lambda} = \mathrm{vol}B_\lambda |A_\lambda|^2 \tag{9}$$

Equation (7) shows that A_λ is essentially a (normalized) Fourier transform of σ_Λ, a fact that we will exploit below. To make this more precise, define the normalized indicator function:

$$I_\lambda(\boldsymbol{x}) = \begin{cases} (\mathrm{vol}B_\lambda)^{-1} & \boldsymbol{x} \in B_\lambda \\ 0 & \text{otherwise} \end{cases} \tag{10}$$

using the fact that the fourier transform (denoted by "~") of a product is the convolution ("*") of the transforms, we obtain

$$A_\lambda(\boldsymbol{k}_r) = \tilde{I}_\lambda(\boldsymbol{k}_r) * \tilde{\sigma}_\Lambda(\boldsymbol{k}_r) \tag{11}$$

$$\tilde{I}_\lambda(\boldsymbol{k}_r) = \frac{1}{\mathrm{vol}B_\lambda} \int_{B_\lambda} e^{i\boldsymbol{k}_r \cdot \boldsymbol{x}} d\boldsymbol{x} \approx \begin{cases} 1 & k_r < \lambda \\ \lambda / k_r & k_r > \lambda \end{cases} \tag{12}$$

(The right-hand side is obtained by using the approximation $e^{i\boldsymbol{k}_r \cdot \boldsymbol{x}} \approx 1$ for $|\boldsymbol{k}_r \cdot \boldsymbol{x}| < 1$, $e^{i\boldsymbol{k}_r \cdot \boldsymbol{x}} \approx 0$ otherwise; more precise expressions depend on the exact shape and dimension of B_λ; for example, the angular part of B_λ is itself the Fourier transform of the antenna shape). Equations (11) and (12) show that A_λ is essentially a "running average" in fourier space over the low frequency modes. Note that in section 3.3 we consider A_λ as a function of the position of the radar pulse, obtaining expressions for the spectrum of spatial variability at a spatial wavevector $\boldsymbol{k}$.

3. The statistics of the effective radar reflectivity factor

3.1 Factorization and the "Hidden" Reflectivity Statistics

For a "conserved cascade," $\sigma(\boldsymbol{x})$ is the direct result of a multiplicative process; hence we have the following factorization [*Schertzer and Lovejoy*, 1987]:

$$\sigma_\Lambda = \sigma_\lambda \left(T_\lambda \sigma_{\Lambda/\lambda} \right) \tag{13}$$

where T_λ is the scale reduction operator (factor $\lambda < \Lambda$; for any function $\sigma(\boldsymbol{x})$ we have by definition $T_\lambda \sigma(\boldsymbol{x}) = \sigma(T_\lambda^{-1} \boldsymbol{x})$; see below). In isotropic systems, $T_\lambda = \lambda^{-1}$; more generally it is given by $T_\lambda = \lambda^{-G}$, where G is the generator of the scale changing group (i.e., in selfsimilar multifractals, $G=I$= the identity). In this paper we consider "linear "GSI"; G is a matrix. Since the volume of the (typically elliptical) ball B changes by $\det T_\lambda = \lambda^{-D}$, where D=Trace G, D is called the "elliptical dimension." The inverse scale ratio corresponding to a vector $\boldsymbol{x}$ will be denoted by the usual notation $|\boldsymbol{x}|$; however now it is equal to the inverse "magnification" ratio required to map $\boldsymbol{x}$ onto the frontier of the unit ball: the scale of the vector $\boldsymbol{x}$ is defined as the value of λ^{-1} for which the vector $T_\lambda^{-1}(\boldsymbol{x})$ is a unit vector. An equivalent, more intuitive definition used below is $|\boldsymbol{x}| = (\mathrm{vol}B_\lambda)^{-1/D}$ where $\boldsymbol{x}$ lies on the border of the ball B_λ.

Since the operator T_λ only acts on the spatial coordinates, in terms of statistics at a fixed point, equation (13) implies the following relation between random variables: $\sigma_\Lambda = \sigma_\lambda \sigma_{\Lambda/\lambda}$. This factorization follows directly from the definition of the multiplicative cascade; see Figure 1 for a schematic diagram. Alternatively, factorization will hold whenever equation (1) holds exactly (it will hold only approximately if there are log corrections to equation (1). In section 3.3 we consider the nonconservative case in which σ_Λ is related to a multiplicative process by a fractional integration.

We now apply factorization first to Z_λ, then to $Z_{e,\lambda}$:

$$Z_\lambda = \sigma_\lambda^2 Z_{\Lambda/\lambda(h)} \tag{14}$$

where $Z_{\Lambda/\lambda(h)}$ is the high-frequency "hidden Z;" hidden from

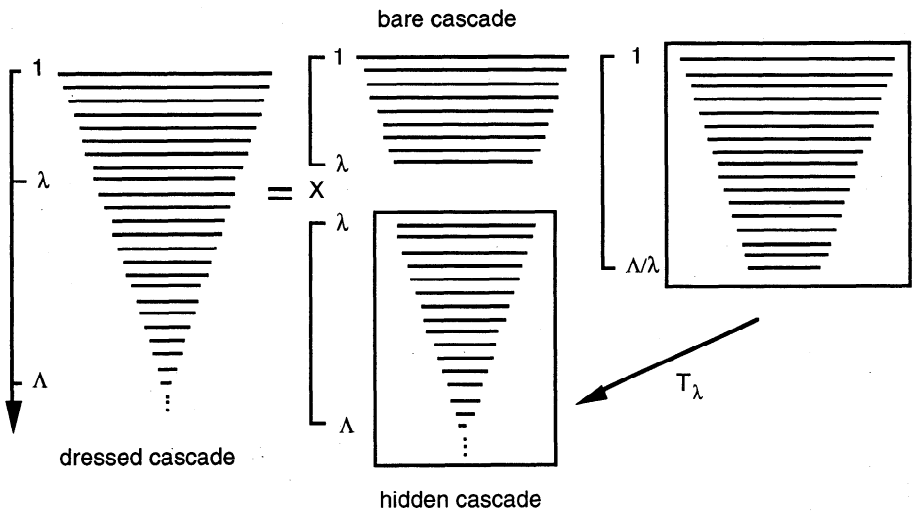

Figure 1 A schematic diagram showing the factorization equation (13). A cascade constructed down to scale ratio Λ, dressed (averaged) up to ratio λ. This is equivalent to a bare cascade constructed over ratio λ, multiplied by a hidden factor obtained by reducing factor λ (the action of the scale changing operator T_λ), a cascade constructed from 1 to Λ/λ.

direct observation by the integration:

$$Z_{\Lambda/\lambda(h)} = \frac{\mathrm{vol}B_\Lambda}{\mathrm{vol}B_\lambda} \int_{B_\lambda} \sigma^2_{\Lambda/\lambda}\left(T_\lambda^{-1}\boldsymbol{x}\right)d\boldsymbol{x} \tag{15}$$

(the term "hidden" is borrowed from renormalization theory [*Schertzer* and *Lovejoy* 1994]).

Similarly, we can consider the statistical properties of $Z_{e,\lambda}$ for scales such that the wavelength is much smaller than the pulse volume (corresponding to typical weather radar parameters). The equations analogous to (14), (15) are:

$$Z_{e,\lambda} = \sigma^2_\lambda Z_{e,\Lambda/\lambda(h)} \tag{16}$$

with

$$Z_{e,\Lambda/\lambda(h)} = \left(\mathrm{vol}B_\lambda\right)^{-1} \int\int_{B_\lambda B_\lambda} \sigma_{\Lambda/\lambda}\left(T_\lambda^{-1}\boldsymbol{x}_1\right)\sigma_{\Lambda/\lambda}\left(T_\lambda^{-1}\boldsymbol{x}_2\right)e^{i\boldsymbol{k}\cdot(\boldsymbol{x}_1-\boldsymbol{x}_2)}d\boldsymbol{x}_1 d\boldsymbol{x}_2 \tag{17}$$

In the appendix we show that for the physically relevant case, $D>K_\sigma(2)$:

$$Z_\lambda \approx \sigma^2_\lambda\left(\mathrm{vol}B_\lambda\right)^{K_\sigma(2)/D}\left(\mathrm{vol}B_\Lambda\right)^{1-K_\sigma(2)/D} = \sigma^2_\lambda \lambda^{-K_\sigma(2)}\Lambda^{-D+K_\sigma(2)} \tag{18}$$

$$Z_{e,\lambda} \approx \sigma^2_\lambda\left(\mathrm{vol}B_\lambda\right)^{K_\sigma(2)/D}\left(\mathrm{vol}B_k\right)^{1-K_\sigma(2)/D} = \sigma^2_\lambda \lambda^{-K_\sigma(2)}k_r^{-D+K_\sigma(2)}$$

We have deliberately written the result in terms of volumes since in the stratified (anisotropic) case, we can conveniently use the relations $k_r=|\boldsymbol{k}_r|=(\mathrm{vol}B_k)^{-1/D}$, $\lambda=(\mathrm{vol}B_\lambda)^{-1/D}$, $\Lambda=(\mathrm{vol}B_\Lambda)^{-1/D}$. To complete the picture, we note the following:

$$\left\langle Z^q_{\lambda,e}\right\rangle \propto \lambda^{K_{Z_e}(q)} \tag{19}$$

$$\left\langle Z^q_\lambda\right\rangle \propto \lambda^{K_Z(q)}$$

with

$$K_{Z_e}(q) = K_Z(q) = K_\sigma(2q) - qK_\sigma(2) \tag{20}$$

Before discussing equation (18), it is interesting to compare it to two other more standard models of subpulse volume variability: the perfectly incoherent and coherent scattering models respectively (details are in the appendix). Table 2 summarizes the various relations derived above for $Z_{e,\lambda}$, Z_λ; they have relatively simple interpretations. The $\sigma_\lambda{}^2$ term is simply due to the large-scale variability and represents the (radar independent) pulse volume scale (natural) variability. We then have a pulse volume dependent factor $\lambda^{-K\sigma(2)}$ absent in the usual theory which is common to both Z, Z_e. This is purely statistical in origin, associated with the scaling of the average of internal multifractal gradients. The expressions for $Z_{e,\lambda}$ and Z_λ differ only in the fact that for $Z_{e,\lambda}$ the inner scale Λ is replaced by the wavelength scale k_r. Considering the effect of the multifractality, since $D>0$, this will result in a change in the reflectivity whenever the rain variability occurs at scales below the wavelength; namely whenever $\Lambda>k_r$. Since Λ^{-1} is of the order of the interdrop distance, this will obviously depend on the rain rate; however, empirical studies have shown that even in moderate rain rates the inner scale can be of the order of a few centimeters, which is smaller than typical wavelengths; the difference should therefore be detectable (see section 4; recall that due to the round trip one should in fact compare twice the waelength to the interdrop distance).

As in the coherent scattering case, the ratio $Z_{e,\lambda}/Z_\lambda$ depends on the ratio $\mathrm{vol}B_k/\mathrm{vol}B_\Lambda$ (assumed >1) raised to a power (1-

Table 2 Various expressions for $Z_{e\lambda}$ and Z

	Incoherent	Coherent	Multifractal
Z_λ	$\sigma_\lambda^2(\mathrm{vol}B_\lambda)$	$\sigma_\lambda^2(\mathrm{vol}B_\lambda)$	$\sigma_\lambda^2(\mathrm{vol}B_\Lambda)^{1-K_\sigma(2)/D}(\mathrm{vol}B_\lambda)^{K_\sigma(2)/D}$
$Z_{e,\lambda}$	Z_λ	$Z_\lambda(\mathrm{vol}B_\Lambda)(\mathrm{vol}B_\lambda)^{-1}\lambda k_r^{-1}$	$Z_\lambda(\mathrm{vol}B_k)^{1-K_\sigma(2)/D}(\mathrm{vol}B_\Lambda)^{-1+K_\sigma(2)/D}$
$Z_{e,\lambda}$	$\sigma_\lambda^2(\mathrm{vol}B_\lambda)$	$\sigma_\lambda^2(\mathrm{vol}B_\lambda)\lambda k_r^{-1}$	$\sigma_\lambda^2(\mathrm{vol}B_\lambda)^{K_\sigma(2)/D}(\mathrm{vol}B_k)^{1-K_\sigma(2)/D}$

The results for the coherent scattering are valid only for isotropic processes, in anisotropic processes the result will depend on the relative orientation of $\boldsymbol{k}_r$.

$K_\sigma(2)/D$) which is >0; that is, the overall effect is for the partial coherence to enhance the effective reflectivity. Observations of clouds (discussed below) show that the liquid water statistics are not so different from those expected for a turbulent passive scalar. In this case σ can be modeled as a fractional integral [*Schertzer and Lovejoy*, 1987, 1991] of a conserved process; see section 3.3.

3.2 Numerical Verification

Using equations (9), (18), we obtain

$$|A_\lambda| = \sigma_\lambda(\mathrm{vol}B_\lambda)^{-1/2+K_\sigma(2)/(2D)}(\mathrm{vol}B_k)^{1/2-K_\sigma(2)/(2D)} \tag{21}$$

by examining the real part of the complex $K_A(q)$ (corresponding to the modulus of A_λ, denoted $K_{A,R}(q)$; see Schertzer and Lovejoy [1995] for complex cascades)

$$K_{A,R}(q) = K_\sigma(q) + \frac{q}{2}(D - K_\sigma(2)) \tag{22}$$

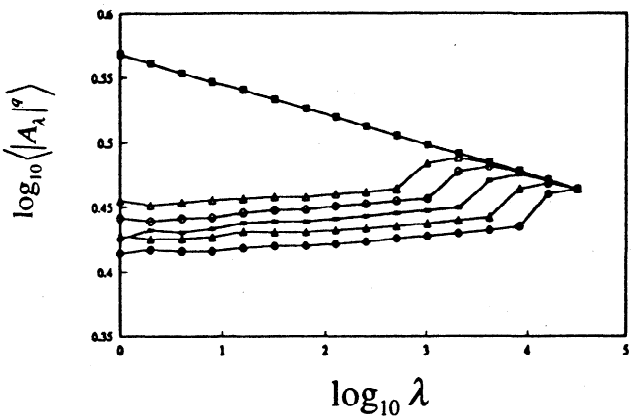

Figure 2a Scaling moments for q = 0.1, computed from simulated lognormal (one dimensional, D=1) multifractals with α=2, C_1 = 0.20, total range of scales, $\Lambda=2^{15}$, 100 stochastic realizations. The top curve is the result for $\langle\sigma_\lambda^q\rangle$; the five bottom curves are for $\langle|A_\lambda|^q\rangle$ with varying wavelengths corresponding to (top to bottom) $k=2^9, 2^{10}, 2^{11}, 2^{12}, 2^{13}$. The jump occurs for $k_r\approx\lambda$, i.e., for wavelengths comparable to pulse lengths; for $k_r>\lambda$ the pulse length is shorter than the wavelength, $\sigma_\lambda \approx |A_\lambda|$, and hence the curves merge. Detailed comparison shows that the spacing between the curves for different wavelengths satisfies equation (21) as expected.

We therefore sought to test the above relation numerically using one-dimensional simulations of continuous cascades [*Schertzer and Lovejoy*, 1987; *Wilson et al.*, 1991; *Pecknold et al.*, 1993; *Pecknold et al.*, 1996]. In this case we used universal multifractals with the following $K_\sigma(q)$:

$$K_\sigma(q) = \begin{cases} \dfrac{C_1(q^\alpha - q)}{\alpha - 1} & \alpha \neq 1 \\ C_1 q Log(q) & \alpha = 1 \end{cases} \tag{23}$$

where $0\le\alpha\le2$ is the Levy index of multifractality and $0\le C_1\le D$ is the codimension of the mean process. Figures 2a, 2b, 2c show a typical result for various scales λ, k_r, and values of q and α which confirms that (except for a short factor ≈4 transition region when $k_r\approx\lambda$) that equation (21) holds quite accurately for $k_r>\lambda$. The jump which occurs for $k_r\approx\lambda$ is because for $k_r<\lambda$, the pulse length is shorter than the wavelength, leading to $\sigma_\lambda \approx |A_\lambda|$, and hence the curves merge as expected. To test equation (22), we note that since $K_\sigma(1)=0$, we obtain $K_\sigma(q)=K_{A,R}(q)-qK_{A,R}(1)$, thus we have

$$\frac{\langle|A_\lambda|^q\rangle}{\langle|A_\lambda|\rangle^q} \approx \langle\sigma_\lambda^q\rangle \tag{24}$$

that is, the normalized modulus $|A_\lambda|/\langle|A_\lambda|\rangle$ has the same scaling properties as σ_λ. We therefore compare the two for

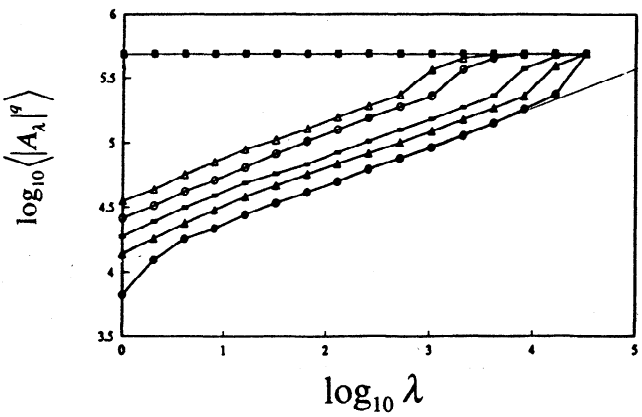

Figure 2b Same as previous except for q = 1, and the wavelengths (top to bottom) are here $k_r=2^9, 2^{10}, 2^{12}, 2^{13}, 2^{14}$. For comparison, we have shown a line with the theoretically predicted slope superimposed on the (bottom) $k_r=2^{14}$ curve.

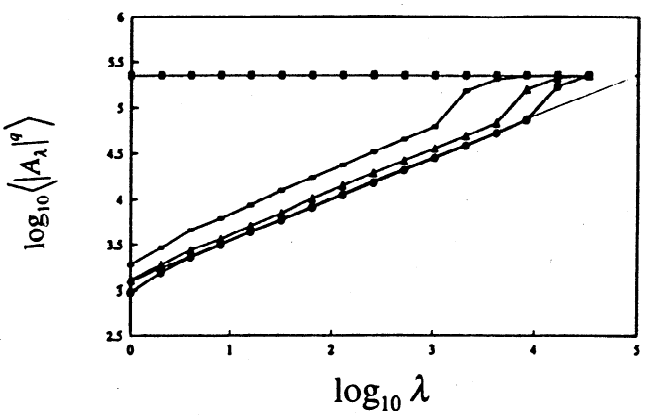

Figure 2c Same as Figures 2a, b except for q = 1, and for universal multifractals with α=1.5, C_1 = 0.06, total range of scales, $\Lambda=2^{15}$. The top curve is the result for $\langle\sigma_\lambda^q\rangle$; the three bottom curves are for $\langle|A_\lambda|^q\rangle$ with varying wavelengths corresponding to (top to bottom) $k=2^{10}$, 2^{12}, 2^{13}. For comparison, we have shown a line with the theoretically predicted slope superimposed on the (bottom) $k_r=2^{13}$ curve.

various values of k_r (figures 3a and 3b). More numerical results can be found in the work of *Duncan* [1993].

3.3. Nonconserved, Fractionally Integrated Fields

In scaling systems, the energy spectrum $E(k)$ at wave number k is of the power law form $E(k)\approx k^{-\beta}$; then β is the spectral exponent. Aircraft measurements of cloud liquid water [*King et al.*, 1981; *Brosamlen*, 1994; *Lovejoy and Schertzer*, 1995a; *Davis et al.*, 1996] indicate that the spectral exponent of liquid water is ≈5/3, the value predicted for passive scalar density fluctuations by the *Corrsin* [1951] and *Obukhov* [1949] theory (a more precise estimate from the latter two references is $\beta\approx1.4$). Since a conservative (multiplicative) process yields $\beta_{con}=1-K(2)$, $K(2)>0$, this indicates that σ cannot be the direct result of a multiplicative process. (This standard relation between β and $K(2)$ can be obtained from the spectral result equation (21) by noting that the energy

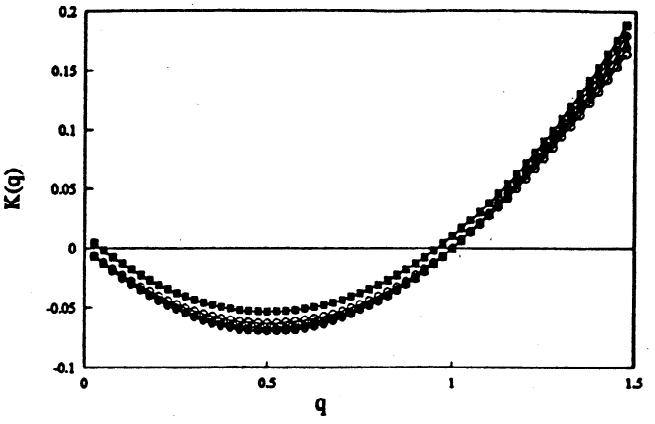

Figure 3a $K_\sigma(q)$ plotted against q along with the corresponding curve for the normalized modulus of A: $(K_{A,R}(q)-qK_{A,R}(1))$ for $k_r=2^{10}$, 2^{11}, 2^{12}, 2^{13}. Same parameters as in Figure 2a. The $K_\sigma(q)$ function for the liquid water field is offset vertically by 0.01 to allow comparison.

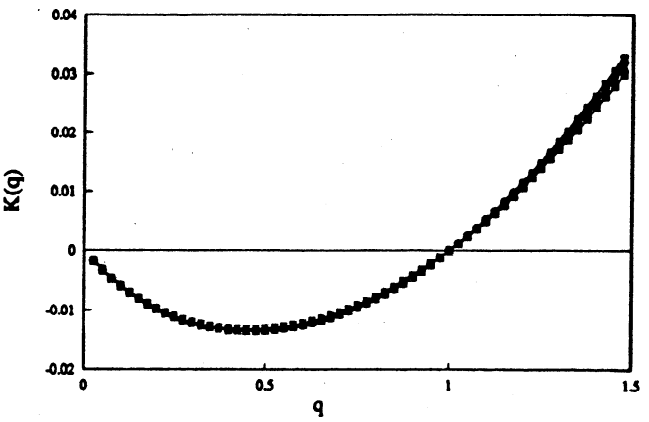

Figure 3b Same as Figure 3a but with the parameters of Figure 2c and for $k_r=2^{10}$, 2^{11}, 2^{12}, 2^{13}.

spectrum is obtained by integrating the fourier modulus squared over all the angles in Fourier space. This angle integration yields an extra factor k^{D-1}). This is not surprising since there is no reason to expect the liquid water density to be conserved. Indeed, passive scalar theory already involves two coupled cascades, of energy flux (ε) and of passive scalar variance flux (χ), with the density fluctuations being determined by the product $\phi=\chi^{3/2}\varepsilon^{-1/2}$: $\sigma_\Lambda=\phi_\Lambda{}^{1/3}\Lambda^{1/3}$. *Schertzer and Lovejoy* [1987] suggested that the extra scaling ($\Lambda^{1/3}$) which is responsible for the increase in β to ≈5/3 corresponds to a fractional integration, i.e., power law filter by $k^{-1/3}$ (hence $\beta=\beta_{con}+2H$). Other related models yielding $\beta>1$ include the "bounded cascade" model [*Cahalan*, 1994] (this is however asymptotically monofractal) and a wavelet-based approach [*Benzi et al.*, 1993]. Considering ϕ_Λ as the conservative process for cloud liquid water, a fractionally integrated field (order H) is

$$\sigma_\Lambda^{(H)}(\boldsymbol{x})=\phi_\Lambda * G_\Lambda \tag{25}$$

with G_Λ the (truncated) fractional integral "Green's function"

$$G_\Lambda(\boldsymbol{x})=\frac{1}{\Gamma(H)}|\boldsymbol{x}|_{[1,\Lambda]}^{H-D} \tag{26}$$

where the subscript on the norm indicates truncation at wavenumbers outside the interval, i.e. in real space, roughly at a small scale Λ^{-1} and a large scale 1; $\Gamma(H)$ is the usual gamma function. This normalization is used since it implies the following Fourier space filter

$$\tilde{\sigma}_\Lambda^{(H)}(\boldsymbol{k})=|\boldsymbol{k}|_{[1,\Lambda]}^{-H}\tilde{\phi}_\Lambda(\boldsymbol{k}) \tag{27}$$

The aircraft results cited above were interpreted as implying $H\approx0.28$ (near the passive scalar value). To understand the effect of fractional integration, it is convenient to consider $A^{(H)}{}_\lambda(\boldsymbol{k}_r,\boldsymbol{x})$, $Z_{e,\lambda}(\boldsymbol{k}_r,\boldsymbol{x})$ $(=|A|^2)$; the amplitude and effective reflectivity factors for pulse volumes $B_\lambda(\boldsymbol{x})$ centered at the point $\boldsymbol{x}$

$$A_\lambda^{(H)}(\boldsymbol{k}_r,\boldsymbol{x})=\frac{1}{\mathrm{vol}B_\lambda(\boldsymbol{x})}\int_{B_\lambda(\boldsymbol{x})}\sigma_\Lambda^{(H)}(\boldsymbol{x}')\left(e^{i\boldsymbol{k}_r\cdot\boldsymbol{x}'}+e^{-i\boldsymbol{k}_r\cdot\boldsymbol{x}'}\right)d\boldsymbol{x}' \tag{28}$$

where we have explicitly included the complex conjugate term. We recognize (see equation (10)) $A^{(H)}{}_{\lambda}(\boldsymbol{k}_r,\boldsymbol{x})$ as the convolution of $I_\lambda(\boldsymbol{x})$ with the integrand, hence using the convolution theorem

$$\tilde{A}_\lambda^{(H)}(\boldsymbol{k}_r,\boldsymbol{k}) = I_\lambda(\boldsymbol{k})\left[\tilde{\sigma}_\Lambda^{(H)}(\boldsymbol{k}-\boldsymbol{k}_r)+\tilde{\sigma}_\Lambda^{(H)}(\boldsymbol{k}+\boldsymbol{k}_r)\right] \tag{29}$$

where we have also used the modulation/translation property of fourier transforms. We now consider two cases of special interest.

1) $|\boldsymbol{k}-\boldsymbol{k}_r| << |\boldsymbol{k}+\boldsymbol{k}_r|$ (if all the components of $\boldsymbol{k}$ and $\boldsymbol{k}_r$ are positive; this includes the high frequency case $|\boldsymbol{k}| \approx |\boldsymbol{k}_r|$). Since generally, $\tilde{\phi}(\boldsymbol{k})$ falls off (on average) algebraically with $|\boldsymbol{k}|$, for $H>0$, we have (using equations (27) and (29))

$$\tilde{A}_\lambda^{(H)}(\boldsymbol{k}_r,\boldsymbol{k}) \approx |\boldsymbol{k}-\boldsymbol{k}_r|_{[1,\Lambda]}^{-H}\tilde{A}_\lambda^{(0)}(\boldsymbol{k}_r,\boldsymbol{k}) \tag{30}$$

This result is relevant to "speckle" and is discussed further below.

2) The low frequency limit; $|\boldsymbol{k}| << |\boldsymbol{k}_r|$. Similarly to case 1), we have:

$$\tilde{A}_\lambda^{(H)}(\boldsymbol{k}_r,\boldsymbol{k}) \approx |\boldsymbol{k}_r|_{[1,\Lambda]}^{-H}\tilde{A}_\lambda^{(0)}(\boldsymbol{k}_r,\boldsymbol{k}) \tag{31}$$

hence for the low frequencies ($|\mathbf{k}| << |\mathbf{k}_r|$), the effect of fractional integration is simply the transformation $A_\lambda \rightarrow k_r^{-H}A_\lambda$ and $Z_{e,\lambda}\rightarrow k_r^{-2H}Z_{e,\lambda}$ that is,

$$Z_{e,\lambda} = \phi_\lambda^2\left(\mathrm{vol}B_\lambda\right)^{K_\phi(2)/D}\left(\mathrm{vol}B_k\right)^{1+(2H-K_\phi(2))/D}$$

$$K_{Z_e}(q) = K_\phi(2q) - 2K_\phi(q) \tag{32}$$

The effect on the high frequencies is discussed in the next subsection.

The problem of evaluating the statistics of Z_λ is much more difficult; it is the problem of a "dressed" fractionally integrated quantity. Essentially, as indicated by *Naud et al.* [1996] (who treats a quite similar problem), the integration smoothes out many of the low-order singularities leaving $K_Z(q)=0$ below a critical moment q_H. To see the difficulty, we can write explicitly

$$Z_\lambda = \frac{\mathrm{vol}B_\Lambda}{\Gamma(H)\mathrm{vol}B_\lambda} \int_{B_1}\int_{B_1}\int_{B_\lambda}\phi_\Lambda^2(\boldsymbol{x})|\boldsymbol{x}-\boldsymbol{x}'|_{[1,\Lambda]}^{H-D}|\boldsymbol{x}-\boldsymbol{x}''|_{[1,\Lambda]}^{H-D}d\boldsymbol{x}d\boldsymbol{x}'d\boldsymbol{x}'' \tag{33}$$

Although higher-order moments are difficult to calculate, the mean is straightforward since $\langle\phi^2\rangle$ is independent of $\boldsymbol{x}$ (ϕ is statistically homogeneous/translationally invariant over B_1). We obtain the following approximation (omitting numerical constants such as $\Gamma(H)$):

$$\langle Z_\lambda\rangle \approx \Lambda^{K_\phi(2)-D} \tag{34}$$

which is independent of λ. Taking the mean of equation (31), we obtain the following bias in the mean:

$$\frac{\langle Z_{e,\lambda}\rangle}{\langle Z_\lambda\rangle} \approx \left(\frac{k_r}{\Lambda}\right)^{K_\phi(2)-D} k_r^{-2H} \tag{35}$$

Note that although the bias in the mean is independent of the pulse volume, this will not generally be true of moments of other orders.

3.4. Multifractal Origin of "Speckle" and Drop Rearrangement Sensitivity

A basic feature of radar signals of rain and surface is that they fluctuate greatly. These fluctuations are perceived in various ways. For example, for radar returns from the surface (fixed targets) this sensitivity is called "speckle" and is associated with great variations in the signal with small changes in look angle or of small (wavelength sized) displacements in radar location. In rain, it is usually perceived (for fixed radars) in the time domain where it has been associated with "drop rearrangement"; that is, the fact that even over milliseconds the relative positions of drops change sufficiently to give large variations of Z_e. We are now in a position to understand the origin of this effect and explain it by using multifractals.

"Speckle" arises because if Z_e is considered a function of position (e.g., of the center of the pulse volume), then a small change in this position ($\boldsymbol{x}$) will lead to a large variation in $Z_{e,\lambda}(\boldsymbol{x})$. To analyze this, recall that for multiplicative processes, both Z and Z_e can be expressed as products of low-frequency factors ($\sigma\lambda^2$) and hidden high-frequency factors. To now, we have been concerned with the low-frequency factors only, studying the behavior at spatial scales of the order of the pulse volume. We now consider the high-frequency variability by considering the hidden factors directly. Specifically, we drop proportionality factors obtaining (cf. equation (A13) with appropriate change of variables)

$$Z_{e,\Lambda/\lambda(h)}(\boldsymbol{x}) \approx \int_{B_\lambda(\boldsymbol{x})}|\boldsymbol{x}'|_{[\lambda,\Lambda]}^{-K_\sigma(2)}e^{i\boldsymbol{k}_r\cdot\boldsymbol{x}'}d\boldsymbol{x}' \tag{36}$$

where $B_\lambda(\boldsymbol{x})$ is the pulse volume centered at the point $\boldsymbol{x}$. The singular algebraic factor of the autocorrelation function for the high frequency factor. The subscript $[\lambda,\Lambda]$ indicates the norm band-limited to wave numbers in the interval $[\lambda,\Lambda]$; for lower frequencies (i.e. $\boldsymbol{x}>\lambda^{-1}$) it is near constant and very small, for high frequencies ($\boldsymbol{x}<\Lambda^{-1}$) it is nearly constant and equal to unity. The translation/modulation property of fourier transforms shows that the effect of the exponential radar phase factor in equation (36) is to shift the singularity from the origin to the radar wavevector $\boldsymbol{k}_r$. Using the indicator function of the pulse volume (equation (12)), and the same approximation as for equation (30) we obtain the Fourier representation of the hidden effective reflectivity factor:

$$\tilde{Z}_{e,\lambda(h)}(\boldsymbol{k},\boldsymbol{k}_r) \approx |\boldsymbol{k}-\boldsymbol{k}_r|_{[\lambda,\Lambda]}^{K_\sigma(2)-D}\tilde{I}_\lambda(\boldsymbol{k}) \tag{37}$$

This equation shows that for $D>K_\sigma(2)$ for $D>K_\sigma(2)$, we obtain a singularity near the radar wave vector $\boldsymbol{k}_r$, indicating rapid variation in $Z_{e,\lambda/\lambda(h)}(\boldsymbol{x})$ on scales near the wavelength scale, the origin of which is precisely the singular multifractal correlations characterized by $K_\sigma(2)$ (note that if the sub-pulse volume were the (monofractal) fractional Brownian motion process, essentially the same behavior would result; see the appendix). This effect is obviously absent in $Z_{\Lambda/\lambda(h)}(\boldsymbol{x})$. Note that since the fourier representation of the effective reflectivity factor ($\tilde{Z}_{e,\lambda}(\boldsymbol{k},\boldsymbol{k}_r)$) is a (smoothing) convolution of the low frequency and high frequency hidden factors, that

the effect of this spectral singularity on $\tilde{Z}_{e,\lambda}(\boldsymbol{k},\boldsymbol{k}_r)$ is somewhat attentuated. However, the basic effect persists for nonconservative processes, since it corresponds to overall multiplication of $\tilde{Z}_{e,\lambda}(\boldsymbol{k},\boldsymbol{k}_r)$ by $|\boldsymbol{k}-\boldsymbol{k}_r|^{-2H}$ (see section 3.3). In practice, this latter singular factor may be more significant for the speckle than that given in equation (37), since it is not affected by a convolution.

For conservative multifractals we can also obtain the equation corresponding to equation (37) for the Fourier transform of the reflectivity factor

$$\tilde{Z}_{\lambda(h)}(\boldsymbol{k}) \approx |\boldsymbol{k}|_{[\lambda,\Lambda]}^{K_\sigma(2,2)-D}\tilde{I}_\lambda(\boldsymbol{k}) \tag{38}$$

where the exponent $K_\sigma(q,\eta)=K_\sigma(q\eta)-qK_\sigma(\eta)$, (i.e., $K_\sigma(2,2)=K_\sigma(4)-2K_\sigma(2)$) is the variance exponent of the spatial average of $\sigma_\Lambda{}^2$. A more revealing comparison between the variability of high-frequency factors is to compare the corresponding energy spectra:

$$\begin{aligned} E_{Z_{e,\Lambda/\lambda(h)}}(\boldsymbol{k}) &\propto \boldsymbol{k}^{D-1}\left\langle\left(\tilde{Z}_{e,\Lambda/\lambda(h)}\right)^2\right\rangle \\ &\approx \boldsymbol{k}^{D-1}\left(\tilde{Z}_{e,\Lambda/\lambda(h)}\right)^2 \end{aligned} \tag{39}$$

(for anisotropic spaces, this is the anisotropic generalization of the usual isotropic spectrum, D is the elliptical dimension; see *Pflug et al* [1991], *Marsan et al* [1996]).

4. Discussion and Conclusions

4.1. Comparison with radar and aircraft data

For conservative (H=0) multifractals we have noted that there are two main effects. The first is common to Z, Z_e and is due to the statistics of the sub pulse volume gradients. It can be quantified by comparing the incoherent scattering Z with the multifractal Z, the enhancement is (from Table 2) the factor $(\lambda/\Lambda)^{K\sigma(2)}=(\eta/l)^{K\sigma(2)}$. The second factor, attributable to partial coherence of the scatters leads to a bias in Z_e with respect to Z

$$Z_e/Z = (\Lambda/k_r)^{D-K\sigma(2)} = (\lambda_w/\eta)^{D-K\sigma(2)}$$

(here and below, we ignore constants of the order of 1; here the factor π). However, in realistic (nonconservative) σ fields, considering the bias in means (equation (32)), there is an extra factor $k_r{}^{-2H}$ (also, $K_\phi(2)$ replaces $K_\sigma(2)$) which is due to the variability over the entire range of cascade scales down to the wavelength scale. We shall see that this is quantitiatively the largest effect and reflects the very different sensitivity of the radar measured Z_e in comparison with the theoretical quantity Z.

We will now estimate this overall bias in the means (e.g. equation (35)). Consider a weather radar with λ_w =10 cm. Direct observations (although limited) [see *Lovejoy and Schertzer*, 1990a] indicate that η is comparable to the inter drop distance and varies inversely with the rain rate, having a value of ≈1 cm in moderate rain. Our assumption $(\lambda_w/\eta)>1$ is therefore likely to be often justified. We now estimate the exponents D, $K_\sigma(2)$. Because of the extreme rain stratification we require elliptical dimensions in the place of the usual ones; empirically [*Lovejoy et al.*, 1987], it has been found that D≈2.22. Assuming that the scaling exponents of liquid water in clouds and in rain are the same, to estimate $K_\phi(2)$, we use the values $K_\phi(2)$≈ 0.15 (deduced from the values in Table 1 of *Lovejoy and Schertzer*, [1995a]). Finally, take η≈1 cm, λ_w=10 cm, thus

$$\left(\frac{k_r}{\Lambda}\right)^{K_\phi(2)-D} \approx 10^2 .$$

Finally, taking the outer scale of the rain process to be ≈10^4 km (i.e., the planetary scale), we obtain $k_r{}^{-2H}$ ≈ $(10^7/10^{-1})^{-0.56} \approx 10^{-5}$. Combining the two factors, we obtain the overall bias ≈10^{-3}.

We should note that the above calculations concentrated on the scaling exponents and ignored constants of the order of 1. Although the overall bias is <<1 (and is presumably quite variable with rain rate) it would not be directly noticed because Z is essentially a theoretical quantity and has never been directly measured (*Lovejoy and Schertzer* [1990a] did however estimate Z, and biases, in a two-dimensional cross section of rain using blotting paper). In any case, weather radar are rarely given absolute (electrical) calibration; rain gage calibration, which involves empirical determination of proportionality factors, would be insensitive to this effect. The main significance of this bias is to underline the inadequacy of Z as a proxy for Z_e in rain meansurements: current radar rain algorithms use theoretical arguments to derive rain rates from Z rather than from the measured Z_e; the two quantities are not even approximately equal.

Finally, we consider the compatibility of equation (32) with the radar multifractal exponents estimated by *Tessier et al.* [1993] and *Lovejoy and Schertzer* [1995b]. First, for universal multifractals, equation (32) predicts that $C_{1Ze}=2^\alpha C_{1\sigma}$, where C_1 is the codimension of the mean and α is the index of multifractality which should be equal for Z_e, σ (see *Tessier et al.* [1993] for more discussion). Using the radar values α=1.4, C_{1Ze}=0.12, we obtain $C_{1\sigma}$=0.05, which is close to the observed value 0.07 [*Lovejoy and Schertzer*, 1995a; *Davis et al.*, 1996]. (It was argued by *Lovejoy and Schertzer* [1995a] that the value of α estimated for cloud liquid water (≈2) was an artifact of the measuring device specifically, because of the difficulty of estimating very low liquid water densities. The estimates of C_1 and higher-order moments are less sensitive to this problem). Another check is afforded by the spectral exponent. From equation (32), we see that the autocorrelation exponent of $Z_{e,\lambda}$ will be $K_\phi(4)-2K_\phi(2)$ (i.e., necessarily >0); we therefore obtain (using the same aircraft estimates of exponents) $\beta_{Ze}=1-K_\phi(4)+2K_\phi(2)$≈0.5. Indeed, equation (28) shows that $Z_{e,\lambda}$ is conservative since $\phi_\lambda{}^2$ is a multiplicative process. This indicates that radar measurements should generally yield spectral exponents <1, a finding consistent with recent radar measurements of ice [*Falco et al.*, 1996]. Empirically, however, the situation is not clear since rather different values of β_{Ze} have been obtained. For example, *Lovejoy and Schertzer* [1995b] show analyses yielding β_{Ze}≈0.3 in the tropics, *Marsan et al* [this issue] find β_{Ze}≈0.9, in midlatitudes, and *Tessier et al.* [1993] find β_{Ze}≈ 1.45 in midlatitudes. Only the former values are <1 and are more or less compatible with the aircraft/theory estimate ≈0.5.

4.2. Conclusions

Growing evidence indicates that rain has structures down to the smallest observed scales which are of the order of the mean interdrop distance which is frequently smaller than radar wavelengths. The simplest hypothesis about the variability

is that the dynamics respect a symmetry principle known as scale invariance. Physically, we are lead to hypothesize a nonlinear mechanism repeating scale after scale (in a stratified/anisotropic manner), building up larger and larger variability from large to small scales. A substantial body of evidence now exists supporting such a view. Other hypotheses are necessarily more complicated because they involve more than one fundamental mechanism (depending on the scale); they should not be adopted unless the simpler scaling hypothesis can be first shown to be inadequate. The standard theory of radar measurements of rain is in fact an extreme example of a nonscaling approach since it assumes that the variability/structures/clustering exist only at scales above the radar resolution becoming homogeneous at subradar scales.

In this paper we have addressed the simplest multifractal radar problem: the relation between the statistics of a multifractal liquid water field and the effective scalar wave reflectivity. We first expressed the problem in terms of a continuous liquid water density field with fixed inner scale of the order of the inter drop distance. The fundamental aspect of the problem is that the radar measures the modulus of a Fourier component of the density; essentially, we need only determine the spectrum of a multifractal. This is quite straightforward. To understand the results, we first considered the simplest case of conservative multifractals and compared three cases for both the reflectivity factor Z and the effective reflectivity factor Z_e: incoherent, coherent, and multifractal sub pulse volume liquid water distributions. The basic results are simple to understand; we obtain, essentially, three effects. The first is the natural pulse volume scale variability (σ_λ^2) which (to within small exponential fluctuations) is the standard result. The second effect is purely statistical (that is, it equally affects Z, Z_e) and is due to the internal pulse-volume gradients; it depends on the pulse volume and the liquid water variance scaling exponent. The final factor is an enhancement of Z_e with respect to Z and depends on the ratio of the wavelength to the inner scale and is the result of partial coherence. We then considered the more realistic case of nonconservative multifractals modeled by fractional integration (order H) of a conservative process. This yielded an additional factor of k_r^{-2H} for $\langle Z_e \rangle$ (but not $\langle Z \rangle$), where k_r is the ratio of the large external scale to the wavelength scale. Using empirical estimates of exponents and scales, we estimate the overall bias as $\approx 10^{-3}$. Although this is $<<1$, it would not be noticed since Z is essentially a theoretical quantity. However, this result does indicate that existing theories which relate rain rate to Z may have little relevance to real radars which measure Z_e. Finally, we examined the high-frequency behavior and showed how multifractals can explain "speckle"/"raindrop rearrangement" variability.

We have stressed that we have only considered the simplest relevant multifractal radar observer's problem: the relation of liquid water and radar statistics. Even in its present scalar wave form, it should apply to a number of systems with volume distributed targets other than rain, such as the radar study of the turbulent dispersion of reflecting chaff. Furthermore, in various surface target problems (such as certain problems connected with the interpretation of synthetic aperture radar images) the problem can be reduced to a distributed target problem of the type solved here; hence our multifractal explanation of "speckle", a consequence of the singular multifractal autocorrelation function, is expected to be quite general. As far as rain is concerned, the major aspect which is missing is the coupling with the velocity field. Without specific assumptions about the velocity/liquid water coupling (presumably via a coupled cascade process as discussed by *Schertzer and Lovejoy* [1987]), no direct conclusions about rain rate measurements can be made. Other extensions include the study of space-time properties (see *Duncan* [1993] for such models of reflectivity, also *Marsan et al.* [this issue], *Tessier et al.* [this issue], and *Over and Gupta* [this issue] for space-time multifractal processes). Finally, extensions of this work to polarization effects in rain and elsewhere require the use of vector waves and tensor dielectrics; the latter to be modeled as tensor multifractals. Such extensions may, for example, explain the observation of multifractal statistics in synthetic aperture radar data of sea ice [*Falco et al.*, 1996].

Appendix

Preliminaries

In this appendix we give details on the calculation of reflectivity statistics for conservative multifractals as well as for pure incoherent and coherent sub pulse models of variability. Starting with equation (15), changing variables ($\boldsymbol{x} = T_\lambda \boldsymbol{x}'$), and recalling that the Jacobian of the transformation is $\det T_\lambda = \lambda^{-D} = \mathrm{vol}B_\lambda$, we obtain

$$Z_{\Lambda/\lambda(h)} = \mathrm{vol}B_\Lambda \int_{B_1} \sigma^2_{\Lambda/\lambda}(\boldsymbol{x}')d\boldsymbol{x}' \tag{A1}$$

As long as this integral converges (see *Schertzer and Lovejoy* [1987; *Schertzer* and *Lovejoy* [1996] for the divergence of moments; empirically, *Lovejoy and Schertzer* [1995a] find convergence of moments of σ less than about 2.3), and for $\Lambda >> \lambda$, the above spatial average is approximately equal to the ensemble average:

$$Z_{\Lambda/\lambda(h)} \approx \mathrm{vol}B_\Lambda \left\langle \sigma^2_{\Lambda/\lambda} \right\rangle = \mathrm{vol}B_\Lambda \left(\frac{\Lambda}{\lambda} \right)^{K_\sigma(2)} \tag{A2}$$

Combining this with equation (14), we obtain:

$$\begin{aligned} Z_\lambda &\approx \sigma^2_\lambda \mathrm{vol}B_\Lambda \left(\frac{\Lambda}{\lambda} \right)^{K_\sigma(2)} \\ &= \sigma^2_\lambda \mathrm{vol}B_\Lambda \left(\mathrm{vol}B_\lambda \right)^{K_\sigma(2)/D} \left(\mathrm{vol}B_\Lambda \right)^{-K_\sigma(2)/D} \end{aligned} \tag{A3}$$

We now consider the statistical properties of $Z_{e,\lambda}$ for scales such that the wavelength is much smaller than the pulse volume (corresponding to typical weather radar parameters). Starting with equations (16) and (17) and by again changing variables ($\boldsymbol{x}_1 = T_\lambda \boldsymbol{x}_1'$, $\boldsymbol{x}_2 = T_\lambda \boldsymbol{x}_2'$), introducing $\Delta\boldsymbol{x} = \boldsymbol{x}_1' - \boldsymbol{x}_2'$, and using the fact that $(T_\lambda^T \boldsymbol{k}) \cdot \boldsymbol{x} = \boldsymbol{k} \cdot (T_\lambda \boldsymbol{x})$, ($T_\lambda^T$ is the transpose of T_λ) and recalling that $\mathrm{vol}(B_1) = 1$, we obtain

$$\begin{aligned} Z_{e,\Lambda/\lambda(h)} = \mathrm{vol}B_\lambda \int_{B_1} \int_{B_1} & \sigma_{\Lambda/\lambda}(\boldsymbol{x}_1') \\ & \sigma_{\Lambda/\lambda}(\boldsymbol{x}_1' - \Delta\boldsymbol{x}) e^{i T_\lambda^T \boldsymbol{k}_r \cdot \Delta\boldsymbol{x}} d\Delta\boldsymbol{x} d\boldsymbol{x}_1' \end{aligned} \tag{A4}$$

We recognize the integral over $\Delta\boldsymbol{x}$ as the Fourier transform of the covariance but with the integral over $\boldsymbol{x}_1'$ implying

spatial rather than ensemble averaging. For $\Lambda>>\lambda$, we expect the spatial and ensemble averages to be nearly equal (once again, as long as the second order moment of σ converges); this approximation will be used below. Note that the exponent involves the reduced wave vector $T_\lambda{}^T\mathbf{k}_r$; for isotropic systems this is simply division by λ.

Incoherent and Coherent Subpulse Volume Scattering

In the case of incoherent scattering we assume the statistics to be multifractal only down to a scale ratio λ; a (finite variance) white noise is assumed below this. To make this explicit, introduce a unit white noise with resolution Λ with density u_Λ. This normalization means that (for all Λ)

$$\int_{B_1}\left\langle u_\Lambda^2\right\rangle d\mathbf{x}=1 \tag{A5}$$

If the field is multifractal down to scale λ, then equation (13) is replaced by

$$\sigma_\Lambda=\sigma_\lambda\left(T_\lambda u_{\Lambda/\lambda}\right) \tag{A6}$$

The correlation structure of the (subpulse volume) noise u_Λ is that of a "δ correlated" field with homogeneity scale Λ, having the following autocorrelation function:

$$\begin{aligned}\left\langle u_\Lambda(\mathbf{x}-\Delta\mathbf{x})u_\Lambda(\mathbf{x})\right\rangle \mathrm{vol}B_\Lambda &= 1 \qquad 0\le|\Delta\mathbf{x}|\le\Lambda^{-1}\\ &= 0 \qquad \Lambda^{-1}\le|\Delta\mathbf{x}|\le 1\end{aligned} \tag{A7}$$

We therefore obtain (replacing the ensemble average by a $\approx$ sign)

$$Z_{e,\Lambda/\lambda(h)}\approx \mathrm{vol}B_\lambda\int_{B_1}\int_{B_{\Lambda/\lambda}}u_{\Lambda/\lambda}^2(\mathbf{x}_1')e^{iT_\lambda^T\mathbf{k}_r\cdot\Delta\mathbf{x}}d\Delta\mathbf{x}d\mathbf{x}_1' \tag{A8}$$

This follows since by equation (A7) the inner integral is nonzero only over $B_{\Lambda/\lambda}$. For $\Lambda>>k_r$, over the ball $B_{\Lambda/\lambda}$ we have $e^{iT_\lambda^T\mathbf{k}_r\cdot\Delta\mathbf{x}}\approx 1$ and hence

$$\int_{B_{\Lambda/\lambda}}e^{iT_\lambda^T\mathbf{k}_r\cdot\Delta\mathbf{x}}d\Delta\mathbf{x}\approx\frac{\mathrm{vol}B_\Lambda}{\mathrm{vol}B_\lambda} \tag{A9}$$

We therefore obtain

$$\begin{aligned}Z_{e,\Lambda/\lambda(h)}&\approx \mathrm{vol}B_\Lambda\int_{B_1}u_{\Lambda/\lambda}^2(\mathbf{x}')d\mathbf{x}'\\ &= Z_{\Lambda/\lambda(h)}\approx\mathrm{vol}B_\Lambda\end{aligned} \tag{A10}$$

which is the usual result (a more refined calculation could be made here to demonstrate that the probability distribution of the fluctuations of the spatial integral about the ensemble mean are in fact exponential, which is the usual radar observer's problem result).

We now perform the calculation for a case of multifractal statistics down to scale λ, coherent scattering involving deterministic homogeneous scatterers with constant density (rather than only stochastic Poisson-distributed scatterers), below this scale (obviously, there is no unique type of coherence which can be considered; this is merely the simplest). In this case for $Z_{\Lambda/\lambda(h)}$ we obtain essentially the same result as before (i.e., $Z_{\Lambda/\lambda(h)}=\mathrm{vol}B_\Lambda$; note the "=" instead of "≈"), whereas for $Z_{e,\lambda/\lambda(h)}$, we use the same autocorrelation equation (A7) but with $\Lambda=1$. The rest of the calculation is the same as the above except that the integral over $B_{\Lambda/\lambda}$ in equations (A8), (A9), (A10) is replaced by an integral over B_1. However, over much of this volume the contribution is negligible, in fact, the significant contribution comes only from the region where $T^T{}_\lambda\mathbf{k}_r\cdot\Delta\mathbf{x}<1$. In fact (see equation (12)), since $k_r>\lambda$, for isotropic spaces, we obtain

$$\int_{B_1}e^{iT_\lambda^T\mathbf{k}_r\cdot\Delta\mathbf{x}}d\Delta\mathbf{x}\approx\frac{\lambda}{k_r} \tag{A11}$$

so that for $Z_{e,\lambda}$, the ratio of the coherent to incoherent scattering is $(\Lambda/k_r)^D\lambda/k_r$.

Multifractal correlations

To obtain the multifractal result corresponding to equation (A10), it suffices to use the following estimate of the multifractal covariance [see e.g. *Monin and Yaglom,* 1975]:

$$\left\langle\sigma_\Lambda(\mathbf{x}-\Delta\mathbf{x})\sigma_\Lambda(\mathbf{x})\right\rangle\approx|\Delta\mathbf{x}|_{[1,\Lambda]}^{-K_\sigma(2)} \tag{A12}$$

(the subscript indicates the cutoffs) using this autocorrelation in equation (A4), and replacing ensemble by spatial averaging, we obtain

$$Z_{e,\Lambda/\lambda(h)}\approx\mathrm{vol}B_\lambda\int_{B_1}|\Delta\mathbf{x}|_{[1,\Lambda/\lambda]}^{-K_\sigma(2)}e^{iT_\lambda^T\mathbf{k}_r\cdot\Delta\mathbf{x}}d\Delta\mathbf{x} \tag{A13}$$

(the use of spatial rather than ensemble averages in the above is a key step; although multifractals are not ergodic, this step is nevertheless justified when the corresponding averages converge, i.e. for moments less than a critical value q_D which we assume; in accord with limited data analyses is >2). Finally, for $D>K_\sigma(2)$, we find using an anisotropic version of standard "Tauberian" theorems [e.g. *Feller*, 1971] relating real and spectral space scaling [see also *Pflug et al.* 1993]

$$\begin{aligned}Z_{e,\Lambda/\lambda(h)}&\approx\mathrm{vol}B_\lambda\left(\frac{\mathrm{vol}B_k}{\mathrm{vol}B_\lambda}\right)^{1-K_\sigma(2)/D}\\ &\approx Z_{\Lambda/\lambda(h)}\left(\frac{\mathrm{vol}B_k}{\mathrm{vol}B_\Lambda}\right)^{1-K_\sigma(2)/D}\end{aligned} \tag{A14}$$

This is the basic result required in section 3.1. Note that the covariance of the (monofractal) fractional Brownian motion (obtained by fractionally integrating gaussian white noise by an amount H) is essentially the same as equation (A12) but with $K_\sigma(2)=2H$. All the hidden factor multifractal results carry over to fractional Brownian motion sub-pulse statistics with this substitution. Note however that the overall model involving a multiplicative cascade down to pulse volume scales but with an additive sub-pulse structure is physically quite artificial.

Acknowledgments. We thank G. L. Austin and P. Schuepp, for discussions and encouragement.

References

Austin, P.M., A Study of the Amplitude Distribution Function for Radar Echoes from Precipitation, Mass. Inst. of Technol., Cambridge 1952.

Benzi, R., L. Biferale, A. Crisanti, G. Paladin, M. Vergassola, and A.

Vulpiani, A random process for the construction of multiaffine fields, *Phys. D 65*, 352-358, 1993.

Brax, P., and R. Pechanski, Levy stable law description on intermittent behaviour and quark-gluon phase transitions, *Phys. Lett. B*, 225-230, 1991.

Brosamlen, G., Radiative transfer in lognormal multifractal clouds and analysis of cloud liquid water data, M.S. thesis, McGill Univ., Montreal, Quebec, Canada, 1994.

Cahalan, R., Bounded cascade clouds: Albedo and effective thickness, *Nonlinear Proc. Geophys.*, *1*, 156-167, 1994.

Corrsin, S., On the spectrum of isotropic temperature fluctuations in an isotropic turbulence, *J. Appl. Phys.*, *22*, 469-473, 1951.

Davis, A., A. Marshak, W. Wiscombe, and R. Cahalan, Scale invariance of liquid water distributions in marine stratocumulus, I, Spectral properties and stationarity issues, J. Atmos. Sci., 53, 1538-1558, 1996.

Duncan, M.R., The universal multifractal nature of radar echo fluctuations, PhD. thesis, McGill Univ., Montreal, Quebec, Canada, 1993.

Duncan, M., S. Lovejoy, F. Fabry, and D. Schertzer, The fluctuating radar cross section (RCS) of multifractal scatterers, *11th Conference on ICCP*, Elsevier, Holland, pp. 997-1000, 1992.

Falco, T., F. Francis, S. Lovejoy, D. Schertzer, B. Kerman, and M. Drinkwater, Scale invariance and universal multifractals in sea ice synthetic aperature radar reflectivity fields, *IEEE Trans. Geosc. Remote Sensing*, *34*, 906-914 1996.

Feller, W., *An Introduction to Probability Theory and Its Applications*, John Wiley, New York, 1971.

Fraedrich, K., and C. Larnder, Scaling regimes of composite rainfall time series, *Tellus*, *45A*, 289-298, 1993.

Gabriel, P., S. Lovejoy, D. Schertzer, and G.L. Austin, Multifractal analysis of resolution dependence in satellite imagery, *Geophys. Res. Lett.*, *15*, 1373-1376, 1988.

Gupta, V.K., and E. Waymire, Multiscaling properties of spatial rainfall and river distribution, *J. Geophys.Res.*, *95*, 1999-2010, 1990.

Gupta, V.K., and E. Waymire, A statistical analysis of mesoscale rainfall as a random cascade, *J. Appl. Meteorol.*, *32*, 251-267, 1993.

Hubert, P., Y. Tessier, P. Ladoy, S. Lovejoy, D. Schertzer, J.P. Carbonnel, S. Violette, I. Desurosne, and F. Schmitt, Multifractals and extreme rainfall events, *Geophys.Res. Lett.*, *20* (10), 931-934, 1993.

Kida, S., Log stable distribution and intermittency of turbulence, *J. Phys. Soc.Jpn.*, *60*, 5-8, 1991.

King, W.D., C.T. Maher, and G.A. Hepburn, Further performance tests on the CSIRO liquid water probe, *J. Appl. Meteorol.*, *20*, 195-202, 1981.

Ladoy, P., F. Schmitt, D. Schertzer, and S. Lovejoy, Variabilité temporelle des observations pluviométriques à Nimes, *C. R. Acad. Sciences*, *317, (II)*, 775-782, 1993.

Lawson, J.L., and G.E. Uhlenbeck, *Threshold Signals*, 388 pp., McGraw-Hill, New York, 1950.

Lhermitte, R.M., and E. Kessler, Estimation of the average intensity of precipitation targets, in *12th Conference on Radio Meteorology*, Am. Meteorol. Soc., Boston, Mass., 1966.

Lovejoy, S., Analysis of rain areas in terms of fractals, in *20th Conference on Radar Meteorology*, pp. 476-484, Am. Meteorol. Soc., Boston, Mass., 1981.

Lovejoy, S., La geometrie fractale des régions de pluie et les simulations aléatoires, *Houille Blanche*, *516*, 431-436, 1983.

Lovejoy, S., and B.B. Mandelbrot, Fractal properties of rain and a fractal model, *Tellus*, *37A*, 209, 1985.

Lovejoy, S., and D. Schertzer, Fractals, rain drops and resolution dependence of rain measurements, *J. Appl. Meteorol.*, *29*, 1167-1170, 1990a.

Lovejoy, S., and D. Schertzer, Multifractals, universality classes and satellite and radar measurements of cloud and rain fields, *J. Geophysi. Res.*, *95*, 2021, 1990b.

Lovejoy, S., and D. Schertzer, Multifractal analysis techniques and the rain and clouds fields from 10^{-1} to 10^{6} m, in *Non-linear Variability in Geophysics: Scaling and Fractals*, edited by D. Schertzer, and S. Lovejoy, pp. 111-144, Kluwer Acad., Norwell, Mass., 1991.

Lovejoy, S., and D. Schertzer, How bright is the coast of Brittany?, in *Fractals in Geoscience and Remote Sensing*, edited by G. Wilkinson, pp. 102-151, Off. for Off. Publ. of the Eur. Commun., Luxembourg, 1995a.

Lovejoy, S., and D. Schertzer, Multifractals and rain, in *New Uncertainty Conceps in Hydrology and Water Ressources*, edited by Z.W. Kunzewicz, pp. 62-103, Cambridge Univ. Press, New York, 1995b.

Lovejoy, S., D. Schertzer, and A.A. Tsonis, Functional box-counting and multiple dimensions in rain, *Science*, *235*, 1036-1038, 1987.

Lovejoy, S., D. Schertzer, P. Silas, Y. Tessier, and D. Lavallée, The unified scaling model of atmospheric dynamics and systematic analysis in cloud radiances, *Ann. Geophys.*, *11*, 119-127, 1993.

Marsan, D., D. Schertzer, and S. Lovejoy, Causal space-time multifractal processes: predictability and forecasting of rain, *J. Geophy. Res., this issue.*

Marshall, J.S., and W. Hitschfeld, Interpretation of the fluctuating echo from random distributed scatterers, I, *Can. J. Physics 31*, 962-994, 1953.

Monin, A. S., and A. M. Yaglom, *Statistical Fluid Mechanics*, M.I.T. Press, Boston, Mass., 1975.

Naud, C., D., Schertzer, and S. Lovejoy, Fractional integration and radiative transfer in multifractal atmospheres, in *Stochastic Models in Geosystems*, edited by W. Woyczynski, and S. Molchansov, *85*, 239-267, Springer-Verlag, New York, 1996.

Obukhov, A., Structure of the temperature field in a turbulent flow, *Izv. Ross. Akad. Nauk. Ser. Geogr. Geofiz*, *13*, 55-69, 1949.

Olsson, J., Limits and characteristics of the multifractal behavior of a high-resolution rainfall time series, *Non-linear Processes in Geophysics*, *2*, 23-29, 1995.

Olsson, J., Validity and applicability of a scale-independent, multifractal relationship for rainfall, *Atmos. Res., in press*, 1996.

Olsson, J. and J. Niemczynowicz, Multifractal analysis of daily spatial rainfall distribntions, *J. of Hydrol., in press*, 1996.

Over, T., and V.J. Gupta, A space-time theory of mesoscale rainfall using random cascades,*J. Geophys. Res., this issue.*

Pecknold, S., S. Lovejoy, D. Schertzer, C. Hooge, and J.F. Malouin, The simulation of universal multifractals, in *Cellular Automata: prospects in astronomy and Astrophysics*, edited by J.M. Perdang, and A. Lejeune, pp. 228-267, World Sci., River Edge, N. J., 1993.

Pecknold, S., S. Lovejoy, and D. Schertzer, The morphology and texture of anisotropic multifractals using generalized scale invariance, in *Stochastic Models in Geosystems*, edited by W. Woyczynski, and S. Molchansov, *85*, 269 - 312, Springer-Verlag, New York, 1996a.

Pecknold, S., S. Lovejoy, D. Schertzer, and C. Hooge, Multifractals and the resolution dependence of remotely sensed data: Generalized Scale Invariance and Geographical Information Systems, in *Scaling in Remote Sensing and Geographical Information Systems*, edited by M.G. D. Quattrochi and M. Goodchild, 361-394, Lewis, Boca Raton, Florida, 1996b.

Pflug, K., S. Lovejoy, and D. Schertzer, Generalized scale invariance, differential rotation and cloud texture, *J. Atmos.Sci.*, *50*, 538-553, 1993.

Rogers, R.R., The effect of variable target reflectivity on weather radar measurements, *Q. J. R. Meteorol.Soc.*, *97*, 154-167, 1971.

Schaffner, M., R. Rhinehart, and R. Leonardi, Detection of nonuniformities within the Radar Measurement Cell, in *19th Radar Conference*, pp. 256-263, Am. Meteorol. Soc., Boston, Mass. 1980.

Schertzer, D., and S. Lovejoy, Generalised scale invariance in turbulent phenomena, *Phys.Chem. Hydrodyn. J.*, *6*, 623-635, 1985.

Schertzer, D., and S. Lovejoy, Physical modeling and analysis of rain and clouds by anisotropic scaling of multiplicative processes, *J.Geophys. Res.*, *92*, 9693-9714, 1987.

Schertzer, D., and S. Lovejoy, Nonlinear variability in geophysics: multifractal analysis and simulation, in *Fractals: Physical Origin and Consequences*, edited by L. Pietronero, pp. 49, Plenum, New York, 1989.

Schertzer, D., and S. Lovejoy, Nonlinear geodynamical variability: multiple singularities, universality and observables, in *Non-linear Variability in Geophysics: Scaling and Fractals*, edited by D. Schertzer, and S. Lovejoy, pp. 41-82, Kluwer Acad., Norwell Mass., 1991.

Schertzer, D., S. Lovejoy, Multifractal Generation of Self-Organized Criticality, in *Fractals In the natural and applied sciences*, edited by M.M. Novak, pp. 325-339, Elsevier, North-Holland, 1994.

Schertzer, D., and S. Lovejoy, From scalar cascades to Lie cascades: Joint multifractal analysis of rain and cloud processes, in *Space/Time Variability and Interdependance for Various Hydrological Processes*, edited by R.A. Feddes, pp. 153-173, Cambridge Univ. Press, New York, 1995.

Schertzer, D. S. Lovejoy, Universal multifractals do exist!, *J. Appl. Meteorol.* in press, 1996a.

Schertzer, D., S. Lovejoy, The multifractal phase transition route to self-organized criticality in turbulence and other dissipative nonlinear systems, *Phys. Reports, (in press)*, 1996b.

Schertzer, D., S. Lovejoy, D. Lavallée, and F. Schmitt, Universal hard multifractal turbulence: Theory and observation, in *Nonlinar Dynamics of Structures*, edited by R.Z. Sagdeyev, U. Frisch, A.S. Moyseyev, and A. Erokhin, pp. 213-235, World Sci., River Edge, N.J., 1991.

Schertzer, D., S. Lovejoy, and F. Schmitt, Structures in turbulence and multifractal universality, in *Small-Scale Structures in 3D and MHD Turbulence*, edited by M. Meneguzzi, A. Pouquet and P. L. Sulem, pp. 137-144., Springer-Verlag, New York, 1995.

Svensson, C., J. Olsson, and R. Berndtsson, Multifractal properties of daily rainfall in two different climates, *Wat. Resourc. Res., 32*, 2463-2472, 1996.

Tessier, Y., Multifractal objective analysis of rain and clouds, Ph.D. thesis, McGill Univ., Montreal, Quebec, Canada, 1993.

Tessier, Y., S. Lovejoy, and D. Schertzer, Universal multifractals: theory and observations for rain and clouds, *J. Appl. Meteorol., 32* (2), 223-250, 1993.

Tessier, Y., S. Lovejoy, P. Hubert, D. Schertzer, and S. Pecknold, Multifractal analysis and modeling of rainfall and river flows and scaling, causal transfer functions, *J. Geophy. Res.*, this isssue 1996.

Torlaschi, E., and R.G. Humphries, Statistics of reflectivity gradients, in *21st Conference on Radar Meteorology*, Am. Meterol. Soc., Boston, Mass., 1983.

Wallace, P.R., Interpretation of the fluctuating echo from random distributed scatterers II, *Can. J. Phys. 31*, 994-1009, 1953.

Wilson, J., D. Schertzer, and S. Lovejoy, Physically based modelling by multiplicative cascade processes, in *Non-linear Variability in Geophysics: Scaling and Fractals*, edited by D. Schertzer, and S. Lovejoy, pp. 185-208, Kluwer Acad., Norwell, Mass., 1991.

S. Lovejoy, M. Duncan, Department of Physics, McGill University, 3600 University Street, Montréal, Québec, H3A 2T8, Canada (e-mail: shaun@physics.mcgill.ca)

D. Schertzer, Laboratoire de Météorologie Dynamique, Université Pierre et Marie Curie, 4 Place Jussieu, boîte 99, F-75252 Cedex 05, France. (e-mail: schertze@lmd.jussieu.fr)

Received December 11, 1995; revised July 10 1996;
accepted July 10, 1996.)